

Topological Difference in 2D Layers Steers the Formation of Rigid and Flexible 3D Supramolecular Isomers: Impact on the Adsorption Properties

Prakash Kanoo,[†] Ryotaro Matsuda,^{‡,§} Ryo Kitaura,[⊥] Susumu Kitagawa,^{*,‡,§,⊥} and Tapas Kumar Maji^{*,†}

[†]Molecular Materials Laboratory, Chemistry and Physics of Materials Unit, Jawaharlal Nehru Centre for Advanced Scientific Research, Jakkur, Bangalore 560 064, India

[‡]Kitagawa Integrated Pore Project, ERATO, JST, Kyoto Research Park, Building 3, Shimogyo-ku, Kyoto 600 8815, Japan

[§]Institute for Integrated Cell-Materials Sciences (iCeMS), Kyoto University, 69 Konoe-cho, Yoshida, Sokyo-ku, Kyoto, Japan

[⊥]Department of Synthetic Chemistry and Biological Chemistry, Graduate School of Engineering, Kyoto University, Katsura, Nishikyo-ku, Kyoto 615 8510, Japan

Supporting Information

ABSTRACT: Starting with the same precursors, pyridine-2,3-dicarboxylate (pyrdc) and 4,4'-bipyridyl (bipy), two 3D porous coordination polymers, $\{[\text{Cu}(\text{bipy})_{0.5}(\text{pyrdc})] \cdot 3\text{H}_2\text{O}\}$ (**1**) and $\{[\text{Cu}(\text{bipy})_{0.5}(\text{pyrdc})] \cdot 0.5\text{bipy} \cdot 3\text{H}_2\text{O}\}$ (**2**), have been synthesized by changing the solvent system from MeOH/H₂O to EtOH/H₂O. Single-crystal structure analysis revealed that **1** and **2** are supramolecular isomers with 3D pillared-layer structures having 1D channel systems. Isomer **1** has a flexible structure and shows gated adsorption behavior, while framework **2** has a rigid backbone and exhibits the adsorption properties of typical microporous materials.

Functional porous coordination polymers (PCPs) or metal–organic frameworks are promising materials because of their high surface area, modifiable pore surface, and tunable pore size.¹ The material properties of PCPs are solely determined by their framework structure, and so there has always been a thrust to fabricate new PCPs by tuning the chemical environment of the pore, which may be useful for advanced material properties, like separation, optoelectronic, sensor, drug delivery, etc.^{2–5} Factors like the temperature, solvent, and reaction stoichiometry greatly influence the process of self-assembly, and it is possible to generate different network superstructures by varying those parameters using the same building units. The fabrication of such diverse network superstructures, a typical phenomenon in coordination polymers known as “supramolecular isomerism” or “polymorphism”, has gained enormous attention because of its advantage in controlling the structural rigidity, flexibility, and regularity, which can modulate the functionality.⁶ Structural rigidity arises from strong metal–ligand binding, which uses linkers having constitutional stiffness or metal clusters as the building units, whereas the flexibility stems from flexible linkers, variable coordination geometry of the metal ions, or guest-induced cooperative movement of the framework on a periodic scale.⁷ In contrast to rigid frameworks, flexible or soft porous frameworks offer ideal platforms for molecular recognition properties, which enhance the selectivity by responding to

specific guest molecules in a particular way.⁸ Although during the past few years there are reports on supramolecular isomerism for a particular metal ion and ligand pair system, to the best of our knowledge, different functional supramolecular isomerisms and their structure–property relationships based on the rigid and flexible structures have yet to be properly accounted for. Here, we report the synthesis, structure, and adsorption properties of two new 3D PCPs, $\{[\text{Cu}(\text{bipy})_{0.5}(\text{pyrdc})] \cdot 3\text{H}_2\text{O}\}$ (**1**) and $\{[\text{Cu}(\text{bipy})_{0.5}(\text{pyrdc})] \cdot 0.5\text{bipy} \cdot 3\text{H}_2\text{O}\}$ (**2**), derived from pyridine-2,3-dicarboxylate (pyrdc) and 4,4'-bipyridyl (bipy) with Cu^{II}. The two frameworks are related by structural isomerism and exhibit different adsorption behaviors with small molecules.

The crystal structures of the compounds were determined from single crystal X-ray diffraction analyses and the geometry around each Cu^{II} atom in **1** and **2** is distorted square pyramidal with a CuO₃N₂ chromophore (Figures 1 and S1 in the Supporting Information, SI). The frameworks of **1** and **2** are made up of 2D nets, constructed of pyrdc and Cu^{II} (Figure 1c,d), and are further pillared by bipy to generate 3D frameworks with water-filled channels (Figures 1e,f and S1, SI). **1** and **2** have similar molecular formulas (if the guest molecules are ignored) and are related as structural isomers. The isomerism arises because of the different binding modes of the 3-carboxy group of pyrdc with Cu^{II} (Figure 1a,b). Each Cu^{II} atom in **1** is bonded to three pyrdc and one bipy ligands. The pyridyl N (N1) and O (O1) atoms of the 2-carboxy group of one of the pyrdc groups are bonded to Cu^{II} in a chelated fashion in the square plane, while the remaining two O-atom coordinations, one in the equatorial plane and the other in the axial plane, are provided by O4 and O4a of the 3-carboxy group from two different pyrdc ligands; the latter are in the μ_2 -O₄ bridging mode with a nearby Cu^{II} center and are responsible for expanding to the 2D net (Figure 1c). The fifth coordination at the axial site is fulfilled by a pyridyl N (N2) atom of bipy, the pyridyl rings of which are at an inclination of 49° to the (010) plane and pillar the 2D nets to construct a 3D pillared-layer

Received: April 4, 2012

Published: August 17, 2012

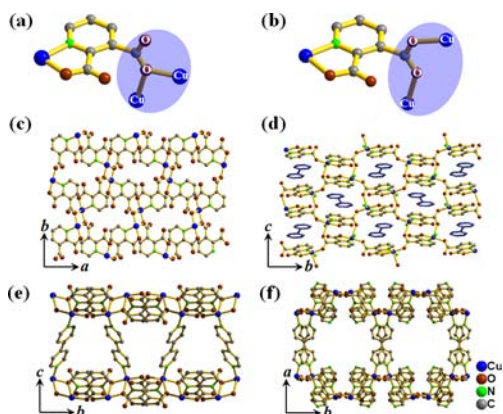


Figure 1. Binding mode of pyrdc with Cu^{II} in **1** (a) and **2** (b). 2D layer formed by Cu^{II} and pyrdc in **1** (c) and **2** (d). View of the 3D pillared-layer frameworks of **1** (e) and **2** (f) showing 1D channels.

framework (Figure 1e). The resultant 3D framework houses a 1D channel ($6.0 \times 4.2 \text{ \AA}^2$; $\sim V_{\text{void}} = 23.4\%$ of the total crystal volume along the crystallographic a axis) occupied by guest water molecules. The coordination environment around Cu^{II} in **2** is similar to that of **1**, except that the 3-carboxy groups of pyrdc bind in a syn-anti bidentate fashion with the two neighboring Cu^{II} centers, resulting in the formation of a 2D corrugated sheet in the bc plane (Figure 1d). The pillars bipy, which steer the 2D nets to construct a 3D framework, are aligned in a criss-cross manner parallel to the c axis. Unlike framework **1**, framework **2** has two different channels, a larger one along the crystallographic c direction, $10 \times 6.8 \text{ \AA}^2$ (Figures 1f and S1 in the SI), and a smaller one, $7.8 \times 1.7 \text{ \AA}^2$, along the crystallographic b direction (Figure S2 in the SI). The channels are occupied by guest water molecules. Besides this, **2** possesses one more channel along an imaginary axis passing through the diagonal of the bc plane and at a distance of $0.5a$, $6.1 \times 3.1 \text{ \AA}^2$, which is occupied by guest bipy molecules (Figure S3 in the SI). The dehydrated framework houses 1175.2 \AA^3 free volume, which is 30.4% of the total crystal volume, as calculated by PLATON.⁹ Topological analyses suggest that the 2D layers in **1** and **2** are different, wherein **1** has a 4-connected net (Schläfli symbol $4^4.6^2$) and **2** has a 3-connected net (Schläfli symbol 4.8^2), and both are uninodal (Figures S4 and S5 in the SI).¹⁰ This difference in the 2D layer topology probably steers the formation of different 3D superstructures in **1** and **2**, resulting in supramolecular isomerism.

Thermogravimetric analyses (TGA) reveal that both compounds are stable up to $210 \text{ }^\circ\text{C}$ after the removal of guest water molecules (Figure S6 in the SI). Although **2** contains guest bipy molecules in its framework, these are not released in this temperature range. This is because the guest bipy molecules in **2** are in strong interaction (π - π and electrostatic) with two different rings (Figure S7 in the SI). The powder X-ray diffraction (PXRD) pattern of the dehydrated compound of **1** (**1'**) shows a shifting of low-angle peaks to higher 2θ value ($8.54^\circ \rightarrow 9.38^\circ$), suggesting structural contraction upon guest removal (Figure S8 in the SI). However, when **1'** is exposed to water vapor, the original framework regenerates. In contrast to **1'**, **2'** exhibits no changes in the peak positions even though it sustains a loss of the guest water molecules, as shown in Figure S9 in the SI. The PXRD study of the PCPs concludes that isomer **1** has a flexible structure, while **2** has a rigid framework.

To unravel the porous properties of compounds **1** and **2**, corresponding dehydrated samples were subjected to adsorption experiments with gas and solvent vapors. N_2 isotherms of **1'** and **2'** measured at 77 K reveal no uptake, suggesting only surface adsorption and no inclusion in the pore (Figure 2).

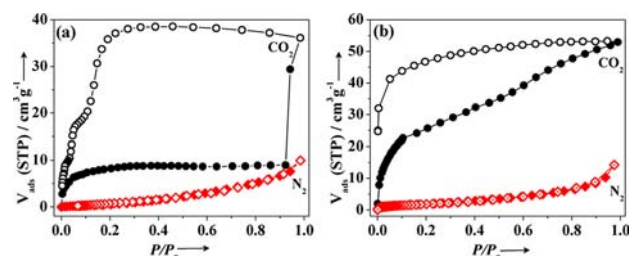
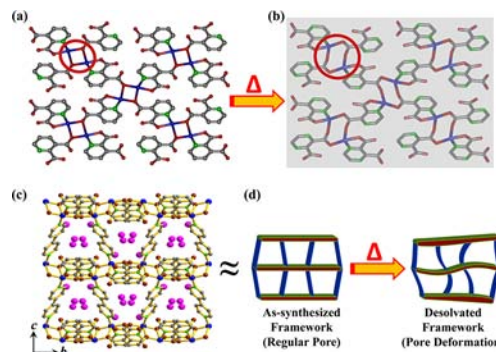


Figure 2. Gas adsorption isotherms for **1'** (a) and **2'** (b): CO_2 (black curves) at 195 K and N_2 (red curves) at 77 K . Closed symbols indicate adsorption and open symbols desorption.

However, quite surprisingly, CO_2 adsorption profiles of the two compounds display completely different behaviors, in contrast to N_2 profiles. The CO_2 adsorption profile of **1'** exhibits unusual behavior with a negligible uptake up to $P/P_0 \approx 0.9$ (Figure 2a). However, at a pressure of about $P/P_0 \approx 0.9$, a steep uptake was observed, suggesting a gate-opening-type behavior and the compound starts to adsorb rapidly with a final uptake value of 38 mL g^{-1} . Interestingly, the profile displays broad hysteresis, retains almost all of the adsorbed CO_2 molecules up to $P/P_0 \approx 0.2$, and then starts to release. To the best of our knowledge, this is the second example of such an observation after that reported by Jooboom et al.¹¹ The gate opening and large hysteresis in the profile can be explained by comparing the PXRD patterns of **1** and **1'**.¹² The PXRD pattern shows a shifting of the (001) peak (this plane contains the 2D layer; Figure S10 in the SI) to a higher 2θ angle in **1'**, indicating structural contraction upon the removal of guest water molecules from **1**. The mechanism of structural contraction upon dehydration has been correlated based on a similar pillared-layer structure of $\{[\text{Cu}_2(\text{pzdc})_2(\text{dpyg})] \cdot 8\text{H}_2\text{O}\}$ (pzdc = pyrazine-2,3-dicarboxylate; dpyg = 1,2-dipyridyl glycol), which has the same topology in the 2D $\{\text{Cu}(\text{pzdc})\}$ layer as that of **1** (Scheme 1 and Figure S8 in the SI).¹³ In the dehydrated structure of $\{[\text{Cu}_2(\text{pzdc})_2(\text{dpyg})] \cdot 8\text{H}_2\text{O}\}$, the neighboring Cu

Scheme 1. Proposed Topology Change in the 2D Layer of 1: (a) As-Synthesized **1**, (b) Desolvated $\{[\text{Cu}_2(\text{pzdc})_2(\text{dpyg})] \cdot 8\text{H}_2\text{O}\}$, (c) 3D Structure with Water-Filled Channels, and (d) Schematic Showing the Change in Pore Structure upon Dehydration



atoms move away from each other by 1.14 Å because of the breaking of the axial Cu–O bond. Instead of single oxygen bridging, now the carboxylate group bridges two Cu atoms via both O atoms (Figure S11c in the SI). We hypothesized that a similar change in the structure 1' would have reduced the space between the 2D layers and hence the window of the 1D channel. As a consequence, in the dehydrated structure, the pores become inaccessible to CO₂ molecules at low pressures. However, because of the highly polar nature of the pore surface, CO₂ molecules with large quadrupole moments interact with the framework strongly and lead to the reopening of the pore structure at high P/P_0 , and hence a gated uptake is observed.

The CO₂ adsorption profile of 2' is shown in Figure 2b, which displays a gradual uptake with increasing pressure, with the final uptake reaching 53 mL g⁻¹. This observation is in stark contrast to the CO₂ profile of 1' and is anticipated. The divergence of the adsorption profiles arises because of the different solid-state behaviors of the frameworks upon desolvation. The different gas adsorption behaviors of the supramolecular isomers can be related to the flexibility and rigidity associated with frameworks 1 and 2 and are unprecedented.

To confirm the structural flexibility and rigidity further, solvent adsorption experiments were carried out at ambient temperature. MeOH profiles show behavior similar to that of CO₂ gas adsorption isotherms (Figure 3). However, because of

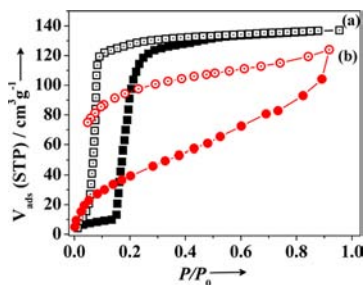


Figure 3. MeOH adsorption profiles of 1' (a) and 2' (b) measured at 293 K. Closed symbols indicate adsorption and open symbols desorption.

the high polarity of MeOH molecules, the gate opens at low pressure, $P/P_0 \approx 0.15$, in the case of 1'. The profile displays a slow increase at the beginning, then increases steeply at $P/P_0 \approx 0.15$, and reaches a saturation value of 137 mL g⁻¹ at $P/P_0 \approx 0.9$. A similar MeOH adsorption profile was also observed in $\{[\text{Cu}_2(\text{pzdc})_2(\text{dpyg})] \cdot 8\text{H}_2\text{O}\}$.¹² In the case of compound 2', however, because of the open-channel structure, the adsorption profile shows a gradual increase with increasing pressure and the final uptake reaches 124 mL g⁻¹ at $P/P_0 \approx 0.9$. Large hysteresis in the MeOH adsorption profiles of 1 and 2 indicates that MeOH molecules interact strongly with the pore surface and desorption, therefore, becomes difficult. H₂O and EtOH adsorption profiles of 1' show behavior similar to that of MeOH; however, the gate-opening pressures are different depending on the size and polarity of the adsorbates (Figure S12 in the SI). Compound 2' shows a gradual uptake of H₂O and EtOH, and both compounds reveal no uptake with 1-PrOH (Figures S12 and S13 in the SI).

In conclusion, we have fabricated two new 3D PCPs using a mixed-ligand system. The use of pyrdoc is limited in the construction of PCPs, and its different binding mode of the 3-carboxy group in two different solvent systems resulted in two different framework structures, related as structural supra-

molecular isomers. The rigidity and flexibility associated with the supramolecular isomers ensues unprecedented adsorption behavior, as observed in the CO₂ and MeOH adsorption studies. The present report thus delineates the functionality of the supramolecular isomers to another level, which was not observed before.

■ ASSOCIATED CONTENT

📄 Supporting Information

Additional figures, TGA, PXRD patterns, and CIF files. This material is available free of charge via the Internet at <http://pubs.acs.org>.

■ AUTHOR INFORMATION

✉ Corresponding Author

*E-mail: tmaji@jncasr.ac.in.

📝 Notes

The authors declare no competing financial interest.

■ ACKNOWLEDGMENTS

The authors are thankful to Lt. Dr. Golam Mostafa for helpful discussions. P.K. acknowledges CSIR, India, for a senior research fellowship.

■ REFERENCES

- (1) Eddaoudi, M.; Kim, J.; Rosi, N.; Vodak, D.; Wachter, J.; O'Keeffe, M.; Yaghi, O. M. *Science* **2002**, *295*, 469.
- (2) (a) Horike, S.; Tanaka, D.; Nakagawa, K.; Kitagawa, S. *Chem. Commun.* **2007**, 3395. (b) Abrahams, B. F.; Moylan, M.; Orchard, S. D.; Robson, R. *Angew. Chem., Int. Ed.* **2003**, *42*, 1848. (c) Maji, T. K.; Matsuda, R.; Kitagawa, S. *Nat. Mater.* **2007**, *6*, 142.
- (3) Wang, C.; Zhang, T.; Lin, W. *Chem. Rev.* **2012**, *112*, 1084.
- (4) (a) Halder, G. J.; Kepert, C. J.; Moubaraki, B.; Murray, K. S.; Cashion, J. D. *Science* **2002**, *298*, 1762. (b) Wadas, T. J.; Wang, Q. M.; Kim, Y. J.; Flaschenreim, C.; Blanton, T. N.; Eisenberg, R. *J. Am. Chem. Soc.* **2004**, *126*, 16841.
- (5) Horcajada, P.; Serre, C.; Maurin, G.; Ramsahye, N. A.; Balas, F.; Vallet-Regi, M.; Sebban, M.; Taulelle, F.; Férey, G. *J. Am. Chem. Soc.* **2008**, *130*, 6774.
- (6) (a) Moulton, B.; Zaworotko, M. J. *Chem. Rev.* **2001**, *101*, 1629. (b) Kishan, M. R.; Tian, J.; Thallapally, P. K.; Fernandez, C. A.; Dalgarno, S. J.; Warren, J. E.; McGrail, B. P.; Atwood, J. L. *Chem. Commun.* **2010**, 46, 538.
- (7) (a) Rosi, N. L.; Eckert, J.; Eddaoudi, M.; Vodak, D. T.; Kim, J.; O'Keeffe, M.; Yaghi, O. M. *Science* **2003**, *300*, 1127. (b) Kanoo, P.; Matsuda, R.; Higuchi, M.; Kitagawa, S.; Maji, T. K. *Chem. Mater.* **2009**, *21*, 5860. (c) Suh, M. P.; Cheon, Y. E.; Lee, E. Y. *Chem.—Eur. J.* **2007**, *13*, 4208.
- (8) (a) Biradha, K.; Hongo, Y.; Fujita, M. *Angew. Chem., Int. Ed.* **2002**, *41*, 3395. (b) Kanoo, P.; Sambhu, R.; Maji, T. K. *Inorg. Chem.* **2011**, *50*, 400. (c) Xiang, S.-C.; Zhang, Z.; Zhao, C.-G.; Hong, K.; Zhao, X.; Ding, D.-R.; Xie, M.-H.; Wu, C.-D.; Das, M. C.; Gill, R.; Thomas, K. M.; Chen, B. *Nat. Commun.* **2011**, *2*, 204.
- (9) Spek, A. L. *J. Appl. Crystallogr.* **2003**, *36*, 7.
- (10) (a) Blatov, V. A.; Carlucci, L.; Ciani, G.; Proserpio, D. M. *CrystEngComm* **2004**, *6*, 377. (b) Blatov, V. A.; Shevchenko, A. P.; Serezhkin, V. N. *J. Appl. Crystallogr.* **2000**, *33*, 1193.
- (11) Seo, J.; Matsuda, R.; Sakamoto, H.; Bonneau, C.; Kitagawa, S. *J. Am. Chem. Soc.* **2009**, *131*, 12792.
- (12) (a) Maji, T. K.; Mostafa, G.; Matsuda, R.; Kitagawa, S. *J. Am. Chem. Soc.* **2005**, *127*, 17152. (b) Kitaura, R.; Fujimoto, K.; Noro, S.; Kondo, M.; Kitagawa, S. *Angew. Chem., Int. Ed.* **2002**, *41*, 133.
- (13) Masaoka, S.; Tanaka, D.; Nakanishi, Y.; Kitagawa, S. *Angew. Chem., Int. Ed.* **2004**, *43*, 2530.